Clinical/Scientific Notes

J.C. DiFrancesco, MD, PhD*
M. Brioschi, MD*
L. Brighina, MD, PhD
C. Ruffmann, MD
E. Saracchi, MD
G. Costantino, MD
G. Galimberti, PhD
E. Conti, PhD
N.A. Curtò, MD
L. Marzorati, MD
P. Remida, MD
F. Tagliavini, MD
M. Savoiardo, MD
C. Ferrarese, MD, PhD

ANTI-Aβ AUTOANTIBODIES IN THE CSF OF A PATIENT WITH CAA-RELATED INFLAMMATION: A CASE REPORT

A 68-year-old man presented with a 4-month history of progressive memory loss and mood disorders. Neurologic examination revealed severe impairment of attention and verbal skills, without motor and sensory deficits. His medical history included mild arterial hypertension, idiopathic partial epilepsy, and obsessive compulsive disorder.

Brain MRI showed the presence of bilateral, asymmetric, swollen white matter lesions in the cerebral hemispheres, hyperintense in T2-weighted images, that partially involved the left frontal cortex (figure). On diffusion-weighted sequences, the white matter abnormalities were consistent with vasogenic edema. No pathologic contrast enhancement was present.

Routine blood tests, inflammatory markers, autoantibodies, neoplastic markers, and paraneoplastic antibodies were within normal limits. CSF examination revealed increased level of proteins (152 mg/dL) and cell count (14 leukocyte/μL), without intrathecal synthesis of oligoclonal bands. Bacterioscopic and virologic tests (including HIV and JCV) were negative, both on CSF and serum. Search for tumor or infection by total body CT scan was negative.

Stereotactic biopsy of the left frontal white matter lesion showed gliosis without signs of infections or neoplasm.

After the biopsy, the patient was treated with dexamethasone 24 mg/day IV for 20 days with marked clinical improvement. A control CSF analysis performed 3 months later was within normal limits (<1 leukocyte/μL, protein 27 mg/dL). Brain MRI demonstrated a reduction in number and extension of the white matter T2-hyperintense lesions (figure). T2*-weighted gradient echo images showed the presence of multiple microhemorrhages scattered over the entire cerebral cortex. No microbleeds were present in basal ganglia, thalami, and posterior fossa (figure).

Diagnosis of probable cerebral amyloid angiopathy–related inflammation (CAA-ri) was made upon clinical and MRI findings, supported by the demonstration of *APOE* ε4 homozygosity.

A search for Aβ deposits in brain tissue and vessel walls on the biopsy sample was negative; a possible explanation is the deep white matter target, with absence of cortex and leptomeninges in the specimen. The Aβ 1-42 protein in the CSF was reduced both in the first (129 pg/mL) and second (125 pg/mL) lumbar puncture compared to normal values (682–1,063 pg/mL). The Aβ 1-40 protein was also investigated (457 pg/mL in the first CSF; 238 pg/mL in the second); however, due to the large variability of this assay as reported in literature, the meaning of these values is unclear.

We hypothesized a spontaneous autoimmune process against CNS Aβ proteins, and assessed the levels of anti-Aβ 1-40 and 1-42 autoantibodies in our patient's CSF, both before and after steroid treatment, compared to 6 age-matched controls (mean age: 63 ± 19 years) and 4 patients with MS (mean age: 45 ± 17 years). We used our ELISA, as described,[1] and detected a marked increase of anti-Aβ 1-40 and 1-42 autoantibodies in the CSF of our CAA-ri patient obtained prior to treatment compared to controls and patients with MS. Interestingly, both autoantibodies were strongly reduced in our case after steroid therapy (figure). As shown in Reiber's graph (figure), this increase is not merely explained by blood–brain barrier damage, but is primarily linked to a specific intrathecal synthesis of anti-Aβ antibodies.

Diagnosis of CAA-ri first requires recognition of CAA.[2,3] CAA is characterized by recurrent lobar hemorrhages without other identified cause and a radiologic pattern often limited to multiple microhemorrhages scattered over the cerebral cortex, with sparing of the basal ganglia and thalami, revealed by T2* gradient echo or susceptibility-weighted images.[3–5] A subgroup of these patients develop vascular inflammation of CAA-affected vessels associated with vasogenic edema shown by T2-hyperintense MRI lesions.

The pathogenesis of CAA-ri is unclear. A predisposing condition to CAA-ri is represented by the *APOE* ε4/ε4 genotype that is present in 80% of patients, compared to 5% with noninflammatory CAA.[4–6] Inflammation could be stimulated by an autoimmune reaction to Aβ occurring spontaneously, in a way otherwise analogous to the development of meningoencephalitis in a subset of patients with Alz-

Editorial, page 772

Figure MRI of cerebral amyloid angiopathy–related inflammation (CAA-ri) and levels of anti-Aβ 1-40 and 1-42 autoantibodies in the CSF

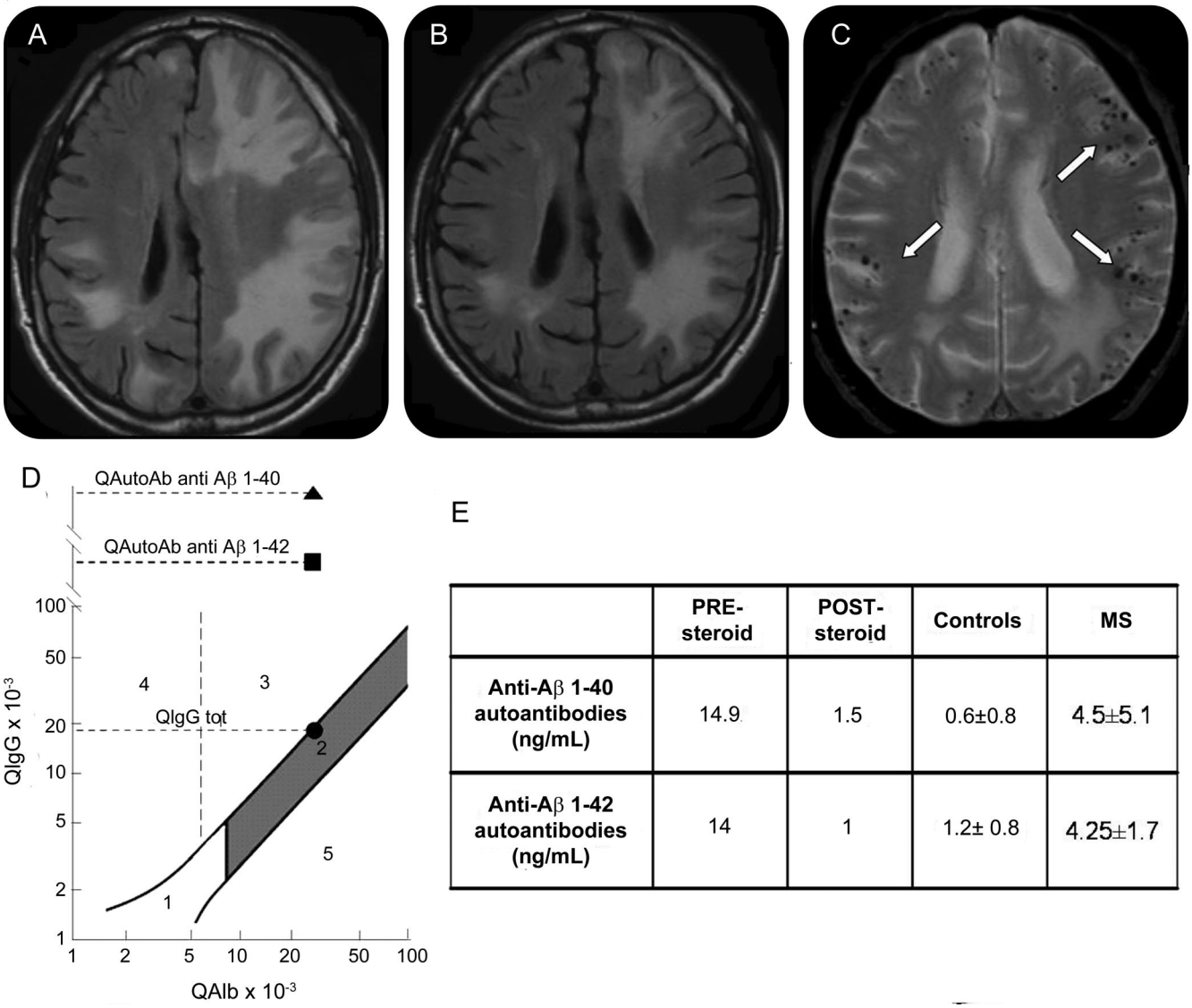

E

	PRE-steroid	POST-steroid	Controls	MS
Anti-Aβ 1-40 autoantibodies (ng/mL)	14.9	1.5	0.6±0.8	4.5±5.1
Anti-Aβ 1-42 autoantibodies (ng/mL)	14	1	1.2± 0.8	4.25±1.7

Axial fluid-attenuated inversion recovery brain MRI shows bilateral hyperintense lesions of the subcortical white matter (A), which are reduced after 20 days of steroid treatment (B). Axial T2*-weighted gradient-echo MRI (C) obtained 33 days later shows further reduction of white matter lesions and multiple, scattered, hypointense cortical lesions due to microhemorrhages (arrows). (D) Reiber's graph. X- and y-axes show, respectively, albumin (QAlb) and immunoglobulin G quotient (QIgG), obtained by the ratio between the level of the protein in the CSF from the first lumbar puncture and in the plasma. The QAlb indicates the permeability of the blood–brain barrier (BBB) to water-soluble molecules. The QIgG (total IgG including specific anti-Aβ autoantibodies) plotted into the graph discriminates between intrathecal production of IgG and increased permeability of the BBB without increased synthesis. Legend of sections: 1 = range of normality, 2 = pure damage of the BBB without intrathecal synthesis, 3 = BBB damage associated to intrathecal synthesis of Ig, 4 = pure intrathecal synthesis without BBB damage, 5 = methodologic fault (in the sample processing or blood withdrawal). The values plotted in the graph (QIgG: 19.7 [circle]; Qanti-Aβ 1-40 autoantibodies: 543 [triangle]; Qanti-Aβ 1-42 autoantibodies: 245.6 [square]) demonstrate both BBB damage and specific intrathecal synthesis of anti-Aβ autoantibodies (section 3). (E) Anti-Aβ 1-40 and 1-42 autoantibodies are increased in the CSF of the CAA-ri patient obtained prior to treatment compared to control subjects and patients with multiple sclerosis. The autoantibodies are strongly reduced after steroid treatment.

heimer disease receiving experimental vaccination to Aβ.[6,7] The dominant component of vascular amyloid deposits in CAA is the short Aβ 1-40. Thus, both autoantibodies against Aβ 1-40 and 1-42 may represent the mediators of the autoimmune reaction occurring in CAA-ri,[6,7] as suggested by our results.

A possible clinical application of our results could be the use of the titer of CSF anti-Aβ antibodies as a biological marker for the diagnosis of CAA-ri. Moreover, since a reduction of autoantibodies was demonstrated after steroid treatment, their measure might also be used to monitor the course of the disease and the efficacy of treatment.

**These authors contributed equally to this work.*

From the Department of Neurology (J.C.D., M.B., L.B., C.R., E.S., G.C., N.A.C., L.M., C.F.), San Gerardo Hospital, University of Milano-Bicocca, Monza; Department of Neuroscience and Biomedical Technologies (J.C.D., M.B., L.B., C.R., E.S., G.C., G.G., E.C., C.F.),

University of Milano-Bicocca, Monza; Neuroradiology Service (P.R.), San Gerardo Hospital, Monza; and Division of Neuropathology (F.T.) and Neuroradiology Department (M.S.), Fondazione Istituto Nazionale Neurologico "Carlo Besta," Milan, Italy.

Disclosure: Dr. DiFrancesco, Dr. Brioschi, and Dr. Brighina report no disclosures. Dr. Ruffmann has received funding for travel from Boehringer Ingelheim and UCB. Dr. Saracchi, Dr. Costantino, Dr. Galimberti, Dr. Conti, Dr. Curtò, Dr. Marzorati, and Dr. Remida report no disclosures. Dr. Tagliavini serves as an Associate Editor for Brain Pathology*, on the editorial board of* Neurological Sciences*, and as Review Editor for* Frontiers in Aging Neuroscience*; and holds a patent re: Discovery of a natural variant of amyloid-β that hinders amyloidogenesis. Dr. Savoiardo and Dr. Ferrarese report no disclosures.*

Received April 8, 2010. Accepted in final form September 7, 2010.

Address correspondence and reprint requests to Dr. Jacopo C. DiFrancesco, Department of Neurology, San Gerardo Hospital, University of Milano-Bicocca, Via Cadore 48, Monza, Italy; jacopo.difrancesco@unimib.it

1. Conti E, Galimberti G, Piazza F, Raggi ME, Ferrarese C. Increased soluble APPalpha, Abeta 1-42, and anti-Abeta 1-42 antibodies in plasma from Down syndrome patients. Alzheimer Dis Assoc Disord 2010;24:96–100.
2. Knudsen KA, Rosand J, Karluk D, Greenberg SM. Clinical diagnosis of cerebral amyloid angiopathy: validation of the Boston criteria. Neurology 2001;56:537–539.
3. Eng JA, Frosch MP, Choi K, Rebeck GW, Greenberg SM. Clinical manifestations of cerebral amyloid angiopathy-related inflammation. Ann Neurol 2004;55:250–256.
4. Kinnecom C, Lev MH, Wendell L, et al. Course of cerebral amyloid angiopathy-related inflammation. Neurology 2007;68:1411–1416.
5. Savoiardo M, Erbetta A, Storchi G, Girotti F. Case 159: cerebral amyloid angiopathy-related inflammation. Radiology 2010;256:323–327.
6. Salloway S, Sperling R, Gilman S, et al. A phase 2 multiple ascending dose trial of bapineuzumab in mild to moderate Alzheimer disease. Neurology 2009;73:2061–2070.
7. Orgogozo JM, Gilman S, Dartigues JF, et al. Subacute meningoencephalitis in a subset of patients with AD after Aβ42 immunization. Neurology 2003;61:46–54.

M.E.C. Meuwissen, MD*
L.S. de Vries, MD, PhD*
H.A. Verbeek, BSc
M.H. Lequin, MD, PhD
P.P. Govaert, MD, PhD
R. Schot, BSc
F.M. Cowan, MD, PhD
R. Hennekam, MD, PhD
P. Rizzu, PhD
F.W. Verheijen, PhD
M.W. Wessels, MD, PhD*
G.M.S. Mancini, MD, PhD*

SPORADIC *COL4A1* MUTATIONS WITH EXTENSIVE PRENATAL PORENCEPHALY RESEMBLING HYDRANENCEPHALY

COL4A1 mutations were initially described in familial porencephaly (OMIM 175780).[1-3] The phenotypic spectrum of *COL4A1* mutations is, however, wide and includes cerebral white matter small vessel disease, cerebral aneurysms, cataract, anterior segment dysgenesis, microcornea, nephropathy, muscle cramps, and cardiac arrhythmia.[4-6] Prenatal onset has been documented.[7] Phenotype–genotype correlation has been proposed for the HANAC phenotype (OMIM 611773).[5]

We report on novel *COL4A1* mutations occurring de novo in 4 Caucasian patients with extensive prenatal brain destruction, adding to the wide phenotypic spectrum.

Methods. *COL4A1* sequencing was performed according to the Dutch regulations for genetic diagnosis.[3] Written informed consent for publication was obtained from the parents.

Case reports. ***Case 1.*** This patient (male) presented antenatally at 27 weeks' gestation with asymmetric ventriculomegaly and extensive cerebral infarction seen on fetal ultrasound and MRI (figure 1, A and B). At birth (37 weeks' gestation), apnea, poor feeding, and seizures developed, leading to death at age 10 days. Postnatal cerebral ultrasound (CUS) and postmortem MRI confirmed severe bilateral ventriculomegaly and tissue atrophy after extensive, putatively deep venous infarctions. Absence of the rostral part of the corpus callosum, a poorly gyrated cortex, and atrophy of the basal ganglia, thalami, brainstem, and cerebellum with an enlarged fourth ventricle were noted (figure 1, C and D). Tortuosity of infratentorial and supratentorial vessels (figure 1C), agenesis of the right kidney, renal artery, and femoral vein and left-sided renal cystic lesions were also seen (figure 1E).

Case 2. This patient (female), born at 40 weeks' gestation, had severe ventriculomegaly and severe cerebellar atrophy seen on fetal ultrasound at 37 weeks' gestation and fetal MRI. Postnatal CUS and MRI confirmed the findings. Susceptibility-weighted imaging (SWI) showed low signal intensity on the ventricular margins suggestive of antenatal hemorrhage (figure 1, F–H). Funduscopy revealed optic atrophy soon after birth. Results of abdominal ultrasound were normal. Progressive high-pressure hydrocephalus developed. She died at 11 weeks.

Case 3. This patient (male) presented with asymmetric ventriculomegaly seen on fetal ultrasound at 26 weeks' gestation. Fetal MRI showed massive cerebral infarction. At birth (40 weeks' gestation) there were apneas and poor feeding; bilateral small corneas and focal central cataracts were noted. Postnatal CUS and MRI showed severe ventriculomegaly and a small cerebellum (figure 1I). MRI 2 years later showed no change in the degree of tissue loss (figure 1J). Results of renal ultrasound were normal. He developed cerebral palsy and seizures.

Case 4. This patient (male), born at 37 weeks' gestation, was very growth-restricted (weight 1,460 g, $\ll$0.4th percentile, and head circumference 27 cm, $<$0.4th percentile). CUS on postnatal day 1 and MRI

Supplemental data at www.neurology.org

Figure 1 MRI

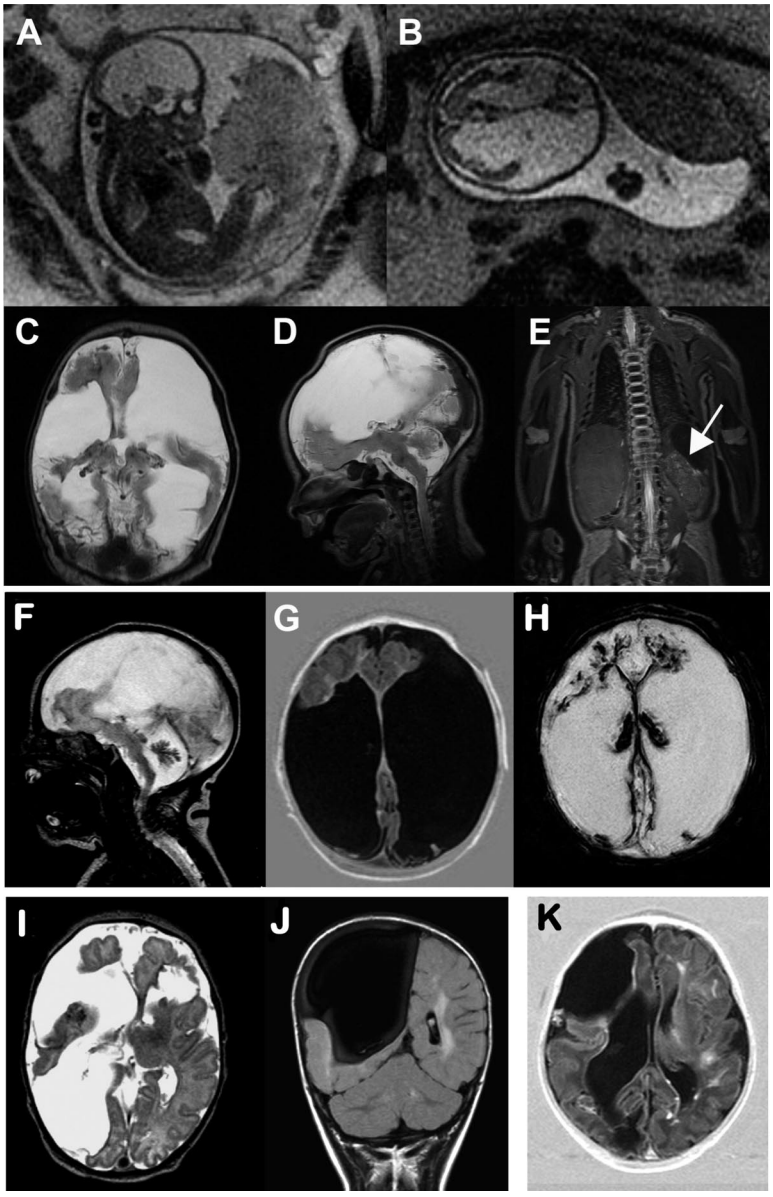

Case 1: fetal MRI at the 28th gestation week. Sagittal (A) and transverse (B) T2-weighed image showing massive cerebral infarction extending to the cortex with loss of gray and white matter. (C, D) T2-weighed images of postmortem brain MRI showing severe bilateral ventriculomegaly with extensive gray and white matter loss, tortuosity of the cerebral arteries, and cerebellar and pontine atrophy. (E) Thoracic and abdominal imaging showing right-sided renal agenesis and multiple small cystic lesions in the left kidney (arrow). Case 2: postnatal sagittal (F) T2-weighted and transverse (G) T1-weighted images showing extensive bilateral infarction as well as severe atrophy of the vermis, pons, and brainstem. The areas of low signal intensity on the susceptibility-weighted image (H) show remnants of old hemorrhage following the venous distribution of the periventricular white matter. Case 3: neonatal transverse T2-weighted images (I) and coronal fluid-attenuated inversion recovery sequence at age 2 years (J), both showing extensive tissue destruction, which is more marked on the right. Case 4: postnatal transverse inversion recovery images (K) showing bilateral porencephaly with cortical destruction. Note the high signal intensity lesions adjacent to the porencephaly and to the lateral ventricles, suggestive of previous hemorrhage.

showed right-sided ventricular dilation with a large cyst adjacent to the right lateral ventricle, an area of cavitation in the left temporal lobe, and a small cerebellum (figure 1K). Bilateral cataracts were noted.

Results of screening for thrombophilia, maternal infection, and anti-rhesus D antibodies in all patients and their mothers were normal.

Results. In patient 1, a heterozygous c.2545G>T mutation (p.G808V) in exon 31 of *COL4A1* was found. Patient 2 harbors a c.2716 + 1G>A splice site mutation in exon 33. In patient 3, a c.3022G>A mutation (p.G1008R) in exon 36 was detected. Patient 4 showed a c.3130G>C mutation (p.G1044R) in exon 37. None of these mutations have been described previously, and they were absent in a panel of 200 ethnically matched control subjects. The 3 glycine substitutions affect highly conserved G-X-Y collagen repeats.[1,2] All mutations were absent in the parents, suggesting de novo events, except for the mother of patient 3, who was found to have a mosaic mutation in the blood. The mutations are located in exons 31, 33, 36, and 37 and are in the same area covering one-fifth of the triple helix domain of the collagen IVα1 protein (figure e-1 on the *Neurology*® Web site at www.neurology.org).

Discussion. The *COL4A1* mutations of our patients are associated with severe encephaloclastic lesions, at first sight resembling hydranencephaly. The type and localization of the lesions may suggest a massive middle cerebral artery territory ischemic stroke, mostly in patients 1 and 3. However, hemosiderin deposits on the ventricular margins from SWI data are more specific for venous infarction and suggest a venous component to the damage in all patients. The pathogenesis could be a massive germinal matrix and intraventricular hemorrhage followed by extensive venous infarction, with compression, edema, and secondary ischemia of large parenchymal areas leading to destruction of the cerebral white matter and cortex and secondary changes in the central gray matter. A similar mechanism could underlie the secondary cerebellar atrophy. However, primary arterial involvement is suggested by the renal agenesis of patient 1 and the previously reported retinal arterial tortuosity and cerebral arterial aneurysms.[2,5,6] Our data show that *COL4A1* testing should also be considered in sporadic severe antenatal hemorrhagic stroke resembling hydranencephaly.

**These authors contributed equally to this work.*

From the Departments of Clinical Genetics (M.E.C.M., H.A.V., R.S., F.W.V., M.W.W., G.M.S.M), Radiology (M.H.L., P.P.G.), and Neonatology (P.P.G.), Erasmus University Medical Center, Rotterdam; Department of Neonatology (L.S.d.V.), Wilhelmina Children's Hospital, University Medical Centre Utrecht, Utrecht, the Netherlands; Department of Paediatrics (F.W.C.), Imperial College Healthcare Trust, London; Great Ormond Street Hospital for Children (R.H.), UCL Institute of Child Health, London, UK; and Department of Paediatrics, Amsterdam Medical Center, and Department of Clinical Genetics, Section of Medical Genomics (P.R.), VU Medical Center, Amsterdam, the Netherlands.

Disclosure: Dr. Meuwissen reports no disclosures. Dr. de Vries serves on the editorial boards of Annals of Neurology, Neuropediatrics, *and the* European Journal of Pediatrics*; receives publishing royalties for* An Atlas of Amplitude: Integrated EEGs in the Newborn, 2nd edition *(Informa Health, 2008) and* An Atlas of Neonatal Brain Sonography, 2nd edition *(MacKeith Press, 2010); and receives research support from the European Union 6th framework programme. H.A. Verbeek, M.H. Lequin, Dr. Govaert, R. Schot, and Dr. Cowan report no disclosures. Dr. Hennekam serves as European Editor of* American Journal of Medical Genetics *and on the editorial boards of* Dutch Scientific Autism Journal, European Journal of Medical Genetics, Genetic Counseling, Lymphatic Research, *and* Molecular Syndromology. *Dr. Rizzu, Dr. Verheijen, Dr. Wessels, and Dr. Mancini report no disclosures.*

Received May 3, 2010. Accepted in final form September 14, 2010.

Address correspondence and reprint requests to Dr. G.M.S. Mancini, Erasmus MC, Department of Clinical Genetics, Postbus 2040, 3000 CA Rotterdam, the Netherlands; g.mancini@erasmusmc.nl

ACKNOWLEDGMENT

The authors thank the patients' families for their collaboration, Dr. Tetsu Teniwa for help obtaining the susceptibility-weighted image, Ruud Koppenol for help with figure 1, and Ronald Grefhorst for providing figure e-1.

1. Gould DB, Phalan FC, Breedveld GJ, et al. Mutations in *COL4A1* cause perinatal cerebral hemorrhage and porencephaly. Science 2005;308:1167–1171.
2. Gould DB, Phalan FC, van Mil SE, et al. Role of *COL4A1* in small-vessel disease and hemorrhagic stroke. N Engl J Med 2006;354:1489–1496.
3. Breedveld G, de Coo IF, Lequin MH, et al. Novel mutations in three families confirm a major role of *COL4A1* in hereditary porencephaly. J Med Genet 2006;43:490–495.
4. Coupry I, Sibon I, Mortemousque B, Rouanet F, Mine M, Goizet C. Ophthalmological features associated with *COL4A1* mutations. Arch Ophthalmol 2010;128:483–489.
5. Plaisier E, Gribouval O, Alamowitch S, et al. *COL4A1* mutations and hereditary angiopathy, nephropathy, aneurysms, and muscle cramps. N Engl J Med 2007;357:2687–2695.
6. van der Knaap MS, Smit LM, Barkhof F, et al. Neonatal porencephaly and adult stroke related to mutations in collagen IV A1. Ann Neurol 2006;59:504–511.
7. de Vries LS, Koopman C, Groenendaal F, et al. *COL4A1* mutation in two preterm siblings with antenatal onset of parenchymal hemorrhage. Ann Neurol 2009;65:12–18.